J Mater Sci: Mater Med (2009) 20:1611–1618
DOI 10.1007/s10856-009-3732-2

The effect of phosphate content on the bioactivity of soda-lime-phosphosilicate glasses

M. D. O'Donnell · S. J. Watts · R. G. Hill · R. V. Law

Received: 9 November 2008 / Accepted: 5 March 2009 / Published online: 28 March 2009
© Springer Science+Business Media, LLC 2009

Abstract We report on the bioactivity of two series of glasses in the SiO_2–Na_2O–CaO–P_2O_5 system after immersion in simulated body fluid (SBF) after 21 days. The effect of P_2O_5 content was examined for compositions containing 0–9.25 mol.% phosphate. Both series of glasses degraded to basic pH, but the solutions tended towards to neutrality with increasing phosphate content; a result of the acidic phosphate buffering the effect of the alkali metal and alkaline earth ions on degradation. Bioactivity was assessed by the appearance of features in the X-ray diffraction (XRD) traces and Fourier transform infrared (FTIR) spectra consistent with crystalline hydroxyl-carbonate-apatite (HCAp): such as the appearance of the (002) Bragg reflection in XRD and splitting of the P–O stretching vibration around 550 cm^{-1} in the FTIR respectively. All glasses formed HCAp in SBF over the time periods studied and the time for formation of this crystalline phase occurred more rapidly in both series as the phosphate contents were increased. For P_2O_5 content >3 mol.% both series exhibited highly crystalline apatite by 16 h immersion in SBF. This indicates that in the compositions studied, phosphate content is more important for bioactivity than network connectivity (NC) of the silicate phase and compositions showing rapid apatite formation are presented, superior to 45S5 Bioglass® which was tested under identical conditions for comparison.

M. D. O'Donnell · S. J. Watts · R. G. Hill
Department of Materials, Imperial College London, London, UK

M. D. O'Donnell · R. V. Law
Department of Chemistry, Imperial College London, London, UK

M. D. O'Donnell (✉)
BioCeramic Therapeutics Ltd., London, UK
e-mail: mdo@bioceramictherapeutics.com

1 Introduction

Bioactive glasses and ceramics have been important for mineralised tissue regeneration in orthopaedic applications for over 30 years [1]. However, recently these materials are finding usage in products such as toothpaste as remineralising agents [2]. The toothpaste Sensishield marketed in the EU by Periproducts contains Novamin (45S5 Bioglass®) as the active ingredient and there is also a toothpaste on the market which contains a zinc substituted hydroxyapatite [3]. L'Oreal also have a patent [4] for Bioglass as an additive to products for relaxing/straightening hair. This opens up the possibility for bioactive glasses to be used in a variety of consumer products.

This study reports the bioactivity of two series of glasses of which structure and properties have been previously reported [5, 6]. In series I phosphate was added to the glass, replacing SiO_2 and the Ca to Na ratio was kept constant. In series II, it was assumed phosphate did not enter the silicate network, but formed a separate orthophosphate phase and sufficient Ca and Na was added to ensure charge neutrality in the PO_4^{3-} complex formed. As the previous study showed, the formation of this type of phosphate structure resulted in removal of network modifiers in series I, polymerising the silicate network and resulting in an increase in Q^3 structural units and a reduction in Q^2. In series II, as sufficient modifier was added to charge balance the orthophosphate species, no change in the silicate structure was seen by solid state NMR; effectively the silicate network remained Q^2, $[Si_nO_{3n}]^{2n-}$ chains of infinite molar mass.

Simulated body fluid (SBF) has been used in vitro in a large number of studies to predict in vivo bioactivity in particular in glass–ceramic systems to assess the formation of hydroxyl-carbonated-apatite at the surface of the material (HCAp). The formation of HCAp after a reasonable time period in SBF is a good indicator that the material will form a bond and integrate well with bone in vivo. Although SBF experiments should be complemented by cell studies, followed by animal and human trials, SBF data can be used to screen out materials for these expensive and possibly unnecessary studies. The glasses studied here are modifications of the original 45S5 Bioglass® composition [1] and glasses studied by Elgayar et al. [7], with phosphate added to investigate the effect on bioactivity. The two most obvious negative effects in vivo might be degradation of the phosphate component of the glass producing an excessively acidic pH and hence cytotoxicity and pyrophosphate (Q^1 phosphate) species producing wide macrophagic activation [8]. It is know that all the glasses in this study contain a separate orthophosphate (Q^0 phosphate) phase. In the compositions studied the degradation and production of acidic pH caused by phosphate would be buffered by the large amount of basic ions (Na and Ca) in the glass and should not result in an acidic pH as seen in polyphosphate glasses [9]. Acidic pH conditions is not desirable for the formation of crystalline apatite. We would not expect the production of pyrophosphate species either as all but one of the glasses studied have a network connectivity (NC) less than 2.5. Typically soda-lime-phosphosilicate glasses with NC >2.5 contain some phosphate in a Q^1 configuration [7, 10].

Compositions are typically designed in weight percentages in the patent literature and also, surprisingly, in the scientific literature. This study avoids that approach as it is difficult to correlate changes in composition with changes in properties. The glasses presented here were designed on a molecular percentage basis. For example in the studies by Gorustovich et al. [11, 12], the authors substituted calcium oxide with strontium oxide on a weight percentage basis. No difference was seen in the two sets of samples in vivo. However, as strontium has a much higher relative atomic mass than calcium, replacing the weight of calcium in the glass with strontium would result in an increase in silica content. This would increase the network connectivity (NC [5, 6]) of the glass, slow dissolution and reduce bioactivity. The beneficial properties of adding the strontium to the glass [13], namely speeding dissolution, promoting osteoblast differentiation and function whilst down-regulating osteoclasts, would be cancelled out by the increase in NC. Therefore it is no surprise no real difference was seen in the calcium bioactive glass compared to the strontium sample in the study by Gorustovich et al.

2 Experimental

The processing of these glasses have been previously reported [5, 6]. Compositions can be found in Table 1 also with network connectivity values assuming phosphate enters the glass network (NC) and that a separate orthophosphate phase is formed (NC′).

2.1 SBF

Simulated body fluid was prepared according to Kokubo and Takadama [14]. Glass particles of diameter <38 μm were immersed in this solution in sealed containers for up to 21 days and were mechanically agitated at 60 rpm using an incubator set to 37°C. At various time points the samples were filtered and dried to constant weight for analysis by XRD and FTIR. Powders were used rather than monoliths as a number of commercial products are supplied in powdered or granular form such as Novabone®, Perioglas® and Vitoss®. The surface area of glass to volume of SBF given in Kokubo method results in problems. For example, for a 5 by 5 mm glass coating on a Ti6Al4V square results in 2.5 ml of SBF, hardly enough to wet the sample.

2.2 XRD

A Phillips powder diffractometer with a copper (Cu K_α) X-ray source (Philips PW 1700 series diffractometer, Philips, Endhoven, NL) was used to characterise the glass samples. The powdered samples were recorded between 10 and 60° 2θ at a scan speed of 0.04° s^{-1}. For crystallite size analysis high resolution scans of the (002) apatite peak

Table 1 Glass compositions used in this study with network connectivity assuming phosphate enters the silicate network (NC) and assuming phosphate forms a separate orthophosphate phase (NC′)

ID	Mol.%				NC	NC′
	SiO_2	Na_2O	CaO	P_2O_5		
Series I						
ICSW1	51.06	26.10	22.84	0.00	2.08	2.08
ICSW2	47.84	26.67	23.33	2.16	2.00	2.18
ICSW3	44.47	27.26	23.85	4.42	1.92	2.30
ICSW5	40.96	27.87	24.39	6.78	1.83	2.44
ICSW4	37.28	28.52	24.95	9.25	1.75	2.62
Series II						
ICSW6	48.98	26.67	23.33	1.02	2.00	2.08
ICSW7	47.07	27.19	23.78	1.95	1.92	2.08
ICSW8	43.66	28.12	24.60	3.62	1.79	2.08
ICSW10	40.71	28.91	25.31	5.07	1.67	2.08
ICSW9	38.14	29.62	25.91	6.33	1.56	2.08

were take between 24 and 28° 2θ for a step size of 0.01°, collecting data on each step for 5 s. Peak analysis was performed using SciDAVis 0.1.3 software.

2.3 FTIR

FTIR spectra were obtained using a Bruker IFS 28 Fourier transform infrared spectrometer in the mid-IR range of 550–2,000 cm^{-1} with a resolution of 0.2 cm^{-1}. Powdered samples were pressed into pellets with KBr. Peak analysis was performed using SciDAVis 0.1.3 software.

3 Results and discussion

3.1 SBF

Figures 1 and 2 shows the variation in pH with time for series I and II glasses respectively after immersion in SBF. As a general trend the SBF becomes more basic with time. This is to be expected as more sodium and calcium ions are released. The solution also shifts towards acidity as the phosphate content of the glasses is increased in both series. This can be explained by the release of more phosphate from the glass which will buffer the alkalinity caused by the sodium and calcium ions. This decrease in pH is advantageous for bioactivity as a pH of $\approx$7.3 is optimal in physiological fluid for apatite deposition [8].

3.2 XRD

Figures 3 and 4 shows XRD traces of selected glasses from series I and II. With progressing time we can see the formation of Bragg peaks associated with apatite crystallisation. The signal to noise of the data is quite low and even after 21 days the apatite formed is relatively disordered. The most prominent features are the Bragg peaks at 25.9° and 31.9° corresponding to the (002) and (211) and reflections [15, 16]. The region containing the (211) peak (30–35°) also contains a number of other features, namely the (112), (300) and (202) reflections [15, 16]. However due to the noise and degree of peak overlap, these lines could not be used for crystallite size analysis. The (002) peak was used for this purpose. Apatite formation can be clearly seen after 16 h. Figure 5 shows the crystallite size obtained from the peak width and position of the 002 peak using the Scherrer equation [17]. After 21 days there is no real variation in the apatite crystallite size. For series II there is possibly a decrease in crystal size with phosphate content, but the variation over the series is less than the error of the peak fitting.

3.3 FTIR

Figures 6 and 7 show FTIR spectra of selected glasses from both series immersed in SBF for up to 21 days. For the glasses containing phosphate, in the 500–600 cm^{-1} region there is a broad feature corresponding to the P–O bending mode and also a Si–O–Si bending vibration in this region [16, 18–20]. Around 720 cm^{-1} in the glass spectra is the band due to Si–O bending vibrations [21, 22]. The dominant bands at approximately 910 and 990 cm^{-1} can be attributed to Si–O (Q^2) and Si–O–Si stretching vibrations respectively [18, 19]. On exposure to SBF, vibrations from the silicate glass network decrease in intensity and bands due to the formation of crystalline hydroxyl-carbonate apatite become dominant. In particular the P–O bend and P–O stretch sharpen and increase intensity at around 580 and 1,010 cm^{-1} respectively [18, 19]. The P–O bend also shows the characteristic splitting indicative of crystalline

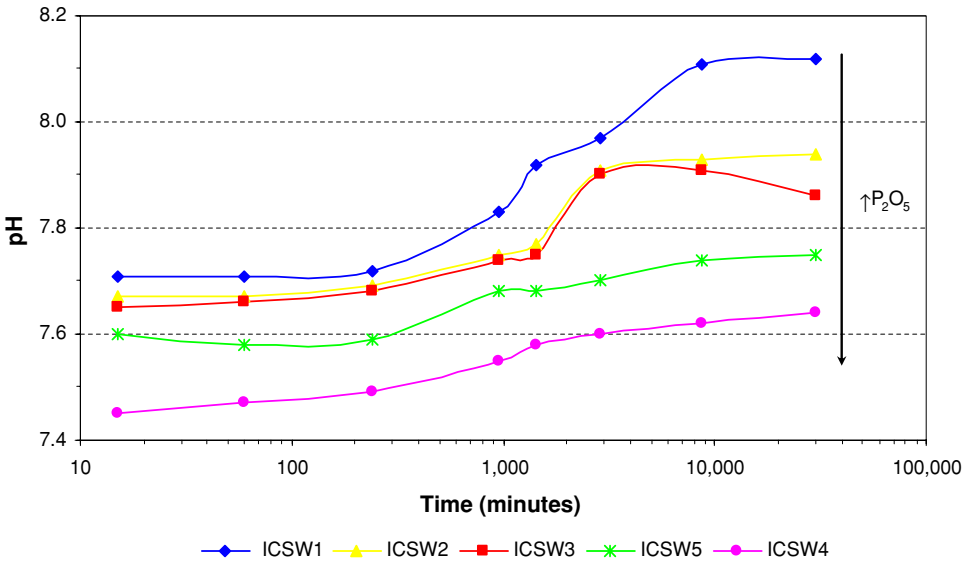

Fig. 1 pH variation of SBF for series I glasses

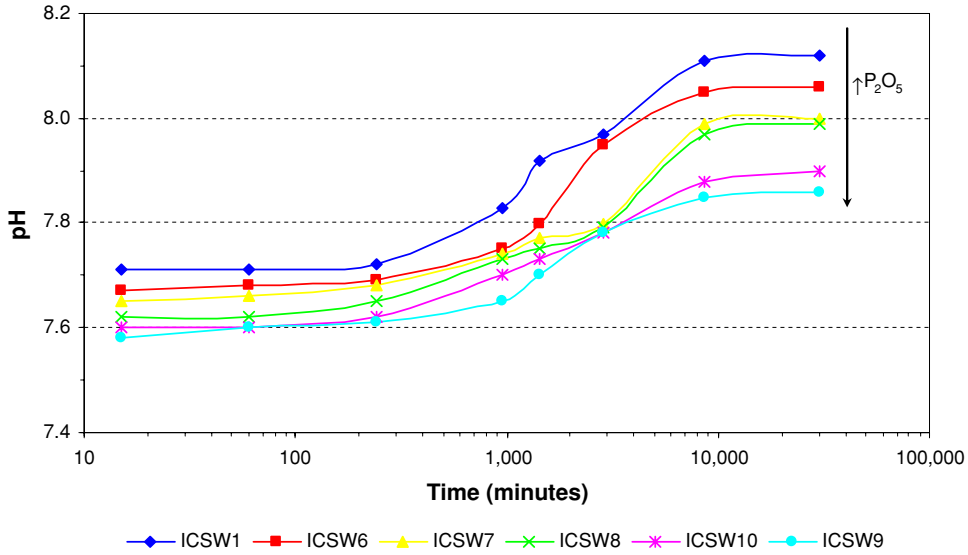

Fig. 2 pH variation of SBF for series II glasses

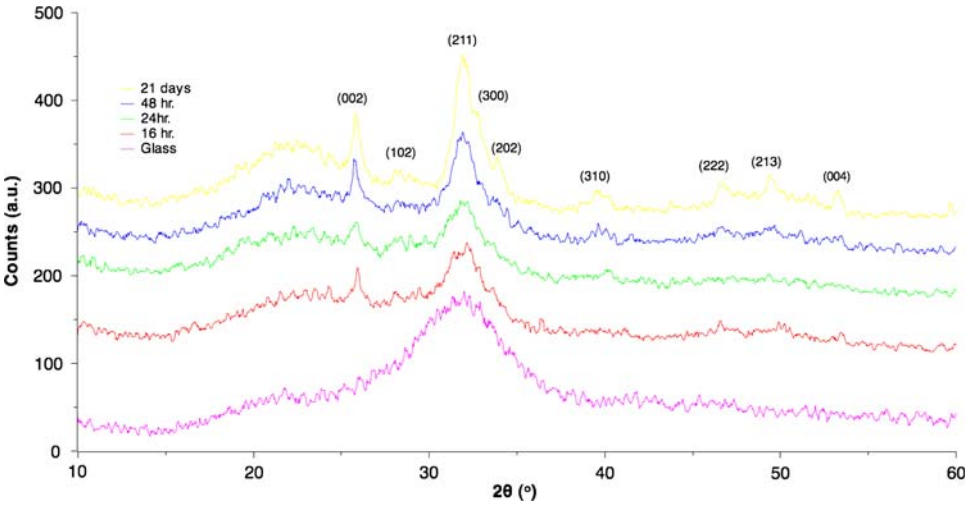

Fig. 3 XRD traces for series I glass ICSW03 (4.42 mol.% P_2O_5) with time of immersion in SBF with the main HCA Bragg peaks labelled

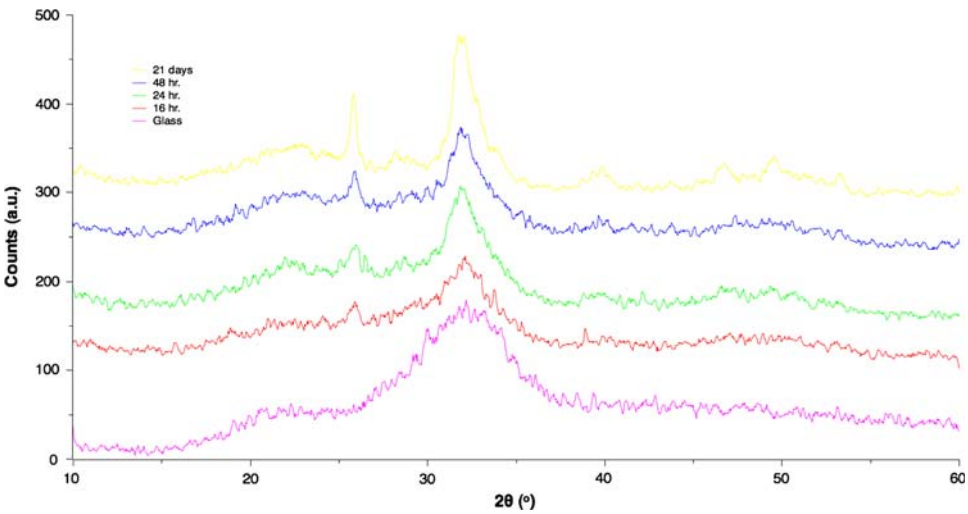

Fig. 4 XRD traces for series II glass ICSW09 (6.33 mol.% P_2O_5) with time of immersion in SBF (see Fig. 3 for Bragg peaks)

apatite formation (into bands at 560 and 600 cm^{-1}) [23]. The appearance of carbonate bands on exposure to SBF is also evidence of crystalline hydroxyl-carbonate-apatite formation with the C–O stretch (v_2) around 860 cm^{-1} and C–O asymmetric stretching (v_3) at 1,410 and 1,450 cm^{-1} [19, 24, 25]. In the samples exposed to SBF the Si–O

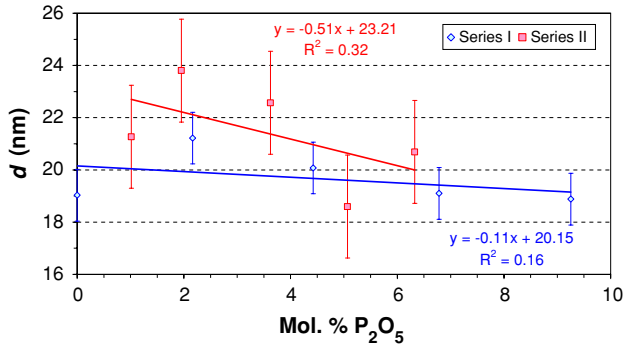

Fig. 5 Crystallite size analysis from 002 Bragg peak for both series of glasses

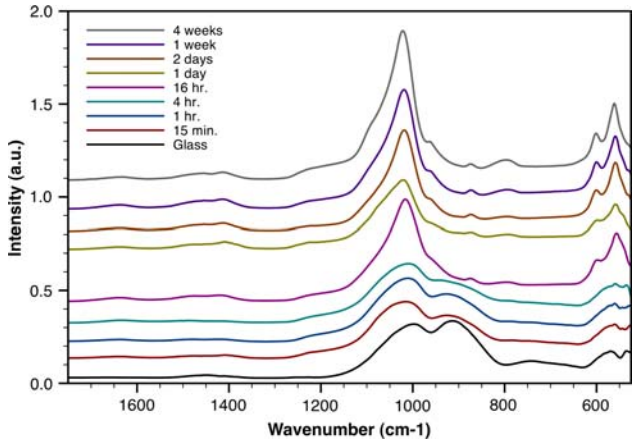

Fig. 6 FTIR spectra of series I glass ICSW05 (6.79 mol.% P_2O_5) with time of immersion in SBF

bending vibration reappears at higher wavenumber ($\approx$800 cm^{-1}) compared to the original glasses which indicates some degree of repolymerisation, possibly condensation of the silica gel formed in the SBF. Serra et al. saw this band shift to higher wavenumber with increasing silica, from 44 to 66 wt%, in bioactive glass samples [22]. The band seen around 1,200 cm^{-1} in the 21 day SBF samples is due to a component of the asymmetric stretching mode of Si–O [22, 26, 27].

3.4 General comments

All glasses showed formation of apatite in the 21 day period tested in SBF. Table 2 summarises the time in which the characteristic splitting of the FTIR P–O bending mode at around 550 cm^{-1} was seen indicating crystalline apatite formation. As a general trend, apatite formation is faster as the phosphate content is increased in the parent glass; even in series I which shows an increase in network connectivity with increasing P_2O_5. This indicates that phosphate content is more important than network connectivity of the silicate phase for bioactivity in the range of compositions studied as long as the phosphate is present as Q^0 species [5, 6]. The glass ICSW4, containing the highest phosphate content in both series does not fit in with the trend shown in Table 2. It is know from previous studies that this sample was partially crystalline [5, 6] which would account for the slower rate of apatite formation compared to the other glasses.

The area of the P–O bending mode (also known as the v_4 phosphate region) can be seen to linearly correlate with the area of the (002) Bragg reflection from XRD as presented in Fig. 8. The areas of these features after 21 days in SBF both increase with phosphate in the parent glass. This indicates that as a general trend, as more phosphate is added to the glasses, more apatite forms which suggests the phosphate content is more important in these two series of glasses than NC for mineralisation even though the network connectivity is increasing in series II and fixed in series II. Also as Fig. 5 shows, the size of the apatite crystals are not varying with phosphate content in the parent glass after 21 days in SBF, but the amount of crystals clearly increases due to the increase in the areas of the features in the XRD and FTIR data associated with HCAp crystallinity. This result is promising, indicating the formation of biomimetic nanocrystalline Ca-deficient hydroxy-carbonate apatite which will bind to proteins such as fibronectin, vitronectin and collagen which encourage osteoblast attachment and proliferation [28].

Figure 9 compares the bioactivity of glass ICSW9 against 45S5 Bioglass® from FTIR spectra taken on glass powders of identical particle sizes exposed to the same SBF conditions. It can clearly be seen that after 1 day in SBF the apatite forms far more rapidly on the ICSW9 glass with intense, narrow, split peaks in the 550 cm^{-1} region, whereas the phosphate peak can hardly be resolved from the background in 45S5. This unequivocally shows the glasses studied here show superior bioactivity and potential as hard tissue remineralising agents compared to 45S5 Bioglass®.

The increased apatite formation could be a result of phase morphology. Pyrex is comprised of sodium borate rich drops in a silica rich matrix. The drops at the glass surface degrade when exposed to corrosive media, however those in the bulk are not affected. Vycor® is another phase separated borosilicate glass. However the borate phase is interconnected and the glass can be etched to form a porous structure. The high phosphate content glasses presented in this study which show increased apatite deposition may exhibit an interconnected orthophosphate morphology resulting in continuous phosphate leaching on exposure to SBF and enhanced apatite formation kinetics. This may be explained by a rapid increase in the surface area of glass exposed to solution in the initial stages of exposure.

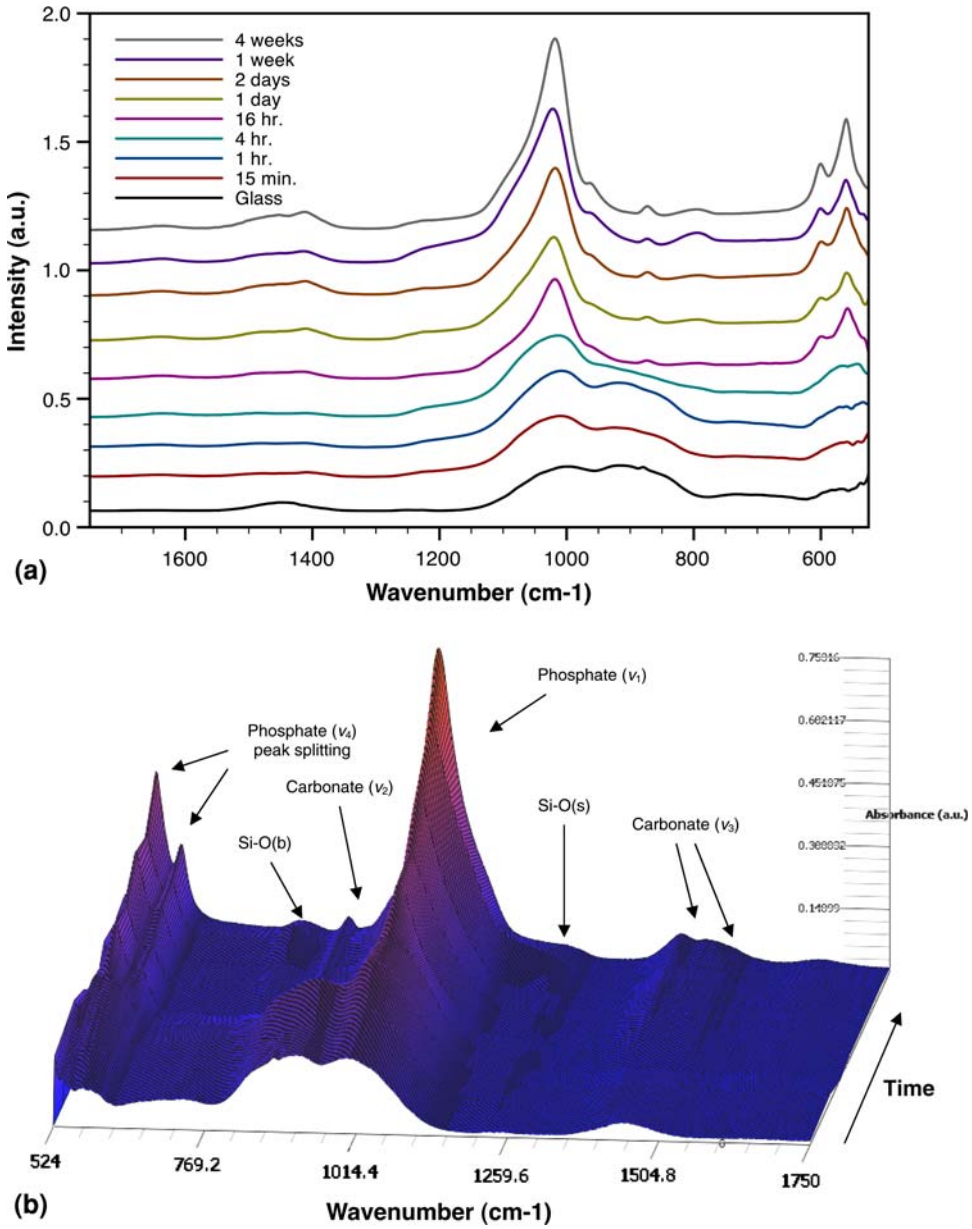

Fig. 7 **a** FTIR spectra of series II glass ICSW10 (5.07 mol.% P_2O_5) with time of immersion in SBF. **b** 3D contour plot (time axis not linear)

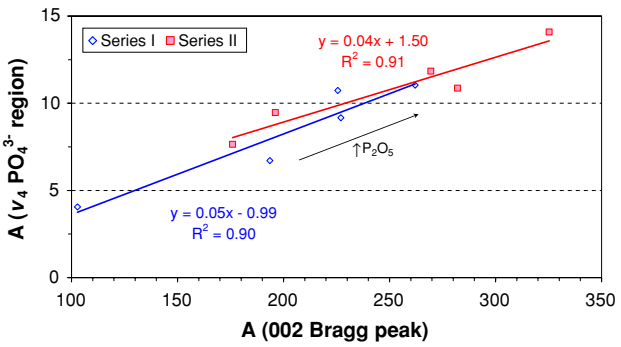

Fig. 8 Area of v_4 phosphate FTIR region plotted against (002) Bragg peak area from XRD after 21 days in SBF

4 Conclusions

In summary, two series of glasses were studied to examine both the effect of network connectivity of the silicate phase and phosphate content on bioactivity. All glasses studied produced a hydroxyl-carbonated-apatite layer on immersion in SBF for up to 21 days. The formation of this layer occurred more rapidly as the phosphate content increased for both series. This is a clear indication that in the compositional ranges studied here, phosphate content is a more important variable than the connectivity of the silicate network or an overriding factor in a process where NC and phosphate dissolution compete. The bioactivity of soda-lime-phosphosilicate glasses can be improved significantly

Table 2 Time for crystalline apatite formation observed by splitting of the FTIR P–O bending mode at around 550 cm^{-1} (sample ICSW4 partially crystalline)

ID	Mol.% P_2O_5	Time
Series I		
ICSW1	0.00	1 week
ICSW2	2.16	2 days
ICSW3	4.42	16 h
ICSW5	6.78	16 h
ICSW4	9.25	1 day[a]
Series II		
ICSW6	1.02	2 days
ICSW7	1.95	2 days
ICSW8	3.62	16 h
ICSW10	5.07	16 h
ICSW9	6.33	16 h

[a] Sample partially crystalline

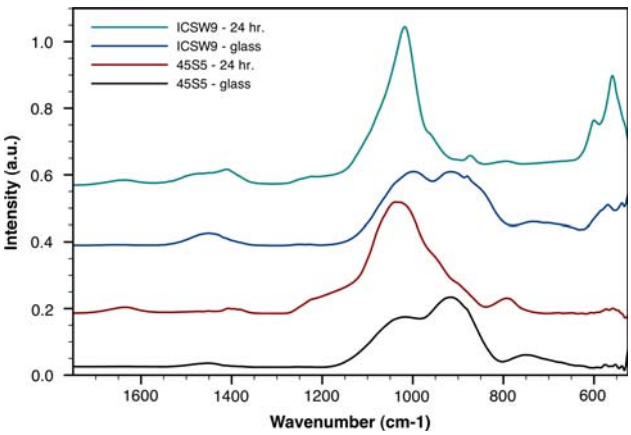

Fig. 9 Comparison of ICSW9 and 45S5 Bioglass® by FTIR after 24 h in SBF

by designing compositions with a good understanding of glass structure.

References

1. Hench LL, Splinter RJ, Allen WC, Greenlee TK. Bonding mechanisms at the interface of ceramic prosthetic materials. J Biomed Mater Res. 1971;5:117–41. doi:10.1002/jbm.820050611.
2. Litkowski LJ, Hack GD, Greenspan DC. Compositions containing bioactive glass and their use in treating tooth hypersensitivity. US Patent 6338751; 2002.
3. Barry JE, Trogolo JA. Antibiotic toothpaste. US Patent 6123925; 2000.
4. Cannell DW, Hashimoto S, Barger KN, Nguyen NV. Hair relaxer compositions comprising a bioactive glass. European Patent EP1709997; 2006.
5. O'Donnell MD, Watts SJ, Law RV, Hill RG. Effect of P_2O_5 content in two series of soda lime phosphosilicate glasses on structure and properties—part I: NMR. J Non-Cryst Solids. 2008;354:3554–60. doi:10.1016/j.jnoncrysol.2008.03.034.
6. O'Donnell MD, Watts SJ, Law RV, Hill RG. Effect of P_2O_5 content in two series of soda lime phosphosilicate glasses on structure and properties—part II: physical properties. J Non-Cryst Solids. 2008;354:3561–6. doi:10.1016/j.jnoncrysol.2008.03.035.
7. Elgayar I, Aliev AE, Boccaccini AR, Hill RG. Structural analysis of bioactive glasses. J Non-Cryst Solids. 2005;351:173–83. doi:10.1016/j.jnoncrysol.2004.07.067.
8. Krajewski A, Ravaglioli A. Bioceramics and biological glasses. In: Barbucci R, editor. Integrated biomaterials science. New York: Kluwer Academic/Plenum; 2002. p. 189–254.
9. Knowles JC. Phosphate based glasses for biomedical applications. J Mater Chem. 2003;10:2395–401. doi:10.1039/b307119g.
10. Grussaute H, Montagne L, Palavit G, Bernard JL. Phosphate speciation in Na2O-CaO-P2O5-SiO2 and Na2O-TiO2-P2O5-SiO2 glasses. J Non-Cryst Solids. 2000;263:312–7. doi:10.1016/S0022-3093(99)00643-2.
11. Gorustovich A, Steimetz T, Cabrini RL, Porto López JM. Osteoconductivity of strontium-doped bioactive glass particles. Bone. 2007;41:S1–13.
12. Gorustovich A, Steimetz T, Porto López JM. Microchemical characterization of bone around strontium-doped bioactive glass particles. Bone. 2007;41:S1–13.
13. Fredholm Y, O'Donnell MD, Kapukhina N, Law RV, Hill RG. Strontium containing bioactive glasses: part 1 glass structure and physical properties. J Non-Cryst Solids (under review).
14. Kokubo T, Takadama H. How useful is SBF in predicting in vivo bone bioactivity? Biomaterials. 2006;27:2907–15. doi:10.1016/j.biomaterials.2006.01.017.
15. Fleet ME, Liu X, King PL. Accommodation of the carbonate ion in apatite: an FTIR and X-ray structure study of crystals synthesized at 2-4 GPa. Am Mineral. 2004;89:1422–32.
16. Vallet-Regí M, Romero AM, Ragel CV, LeGeros RZ. XRD, SEM-EDS, and FTIR studies of in vitro growth of an apatite-like layer on sol-gel glasses. J Biomed Mater Res A. 1999;44:416–21. doi:10.1002/(SICI)1097-4636(19990315)44:4<416::AID-JBM7>3.0.CO;2-S.
17. Cullity BD. Elements of X-ray diffraction. Reading, MA: Addison-Wesley; 1956.
18. Regina M, Filgueiras T, La Torre G, Hench LL. Solution effects on the surface reactions of three bioactive glass compositions. J Biomed Mater Res. 1993;27:1485–93. doi:10.1002/jbm.820271204.
19. Peitl O, Dutra Zanotto E, Hench LL. Highly bioactive P_2O_5-Na_2O-CaO-SiO_2 glass-ceramics. J Non-Cryst Solids. 2001;292:115–26. doi:10.1016/S0022-3093(01)00822-5.
20. Filho OP, La Torre GP, Hench LL. Effect of crystallization on apatite-layer formation of bioactive glass 45S5. J Biomed Mater Res A. 1996;30:509–14. doi:10.1002/(SICI)1097-4636(199604)30:4<509::AID-JBM9>3.0.CO;2-T.
21. Sanders DM, Person WB, Hench LL. Quantitative analysis of glass structure with the use of infrared reflection spectra. Appl Spectrosc. 1974;28:247–55. doi:10.1366/000370274774332623.
22. Serra J, González P, Liste S, Serra C, Chiussi S, León B, et al. FTIR and XPS studies of bioactive silica based glasses. J Non-Cryst Solids. 2003;332:20–7. doi:10.1016/j.jnoncrysol.2003.09.013.
23. Penel G, Leroy G, Rey C, Sombret B, Huvenne JP, Bres E. Infrared and Raman microspectrometry study of fluor-fluor-hydroxy and hydroxy-apatite powders. J Mater Sci Mater Med. 1997;8:271–6. doi:10.1023/A:1018504126866.
24. Santos RV, Clayton RN. The carbonate content in high-temperature apatite; an analytical method applied to apatite from the Jacupiranga alkaline complex. Am Mineral. 1995;80:336–44.

25. Rey C, Collins B, Goehl T, Dickson I, Glimcher M. The carbonate environment in bone mineral: a resolution-enhanced fourier transform infrared spectroscopy study. Calcif Tissue Int. 1989;45:157–64. doi:10.1007/BF02556059.
26. Galeener FL, Lucovsky G. Longitudinal optical vibrations in glasses: GeO_2 and SiO_2. Phys Rev Lett. 1976;37:1474. doi:10.1103/PhysRevLett.37.1474.
27. Lange P. Evidence for disorder-induced vibrational mode coupling in thin amorphous SiO_2 films. J Appl Phys. 1989;66:201–4. doi:10.1063/1.344472.
28. Vallet-Regi M, Arcos D. Biomimetic nanoceramics for clinical use. Cambridge: RSC Publishing; 2008.